PNNL-13003

Pacific Northwest
National Laboratory
Operated by Battelle for the
U.S. Department of Energy

PNNL/Euratom Glass Fiber Optic, Spent Fuel Neutron Profile Measurement System

S.M. Bowyer
John E. Smart

September 1999

Prepared for the U.S. Department of Energy
under Contract DE-AC06-76RLO 1830

DISCLAIMER

PACIFIC NORTHWEST NATIONAL LABORATORY
operated by
BATTELLE
for the
UNITED STATES DEPARTMENT OF ENERGY
under Contract DE-AC06-76RLO 1830

Printed in the United States of America

Available to DOE and DOE contractors from the Office of Scientific and Technical Information, P.O. Box 62, Oak Ridge, TN 37831; prices available from (615) 576-8401.

Available to the public from the National Technical Information Service, U.S. Department of Commerce, 5285 Port Royal Rd., Springfield, VA 22161

This document was printed on recycled paper.
(9/97)

DISCLAIMER

Portions of this document may be illegible in electronic image products. Images are produced from the best available original document.

PNNL- 13003

PNNL/Euratom Glass Fiber Optic, Spent Fuel Neutron Profile Measurement System

Sonya M. Bowyer
John E. Smart

September 1999

Pacific Northwest National Laboratory
Richland, Washington 99352

Summary

Discussions between Euratom and PNNL revealed a need for a neutron detection system that could measure the neutron profile down the entire length of a CASTOR in one measurement. The CASTORS (dry storage casks for spent fuel and vitrified wastes) are roughly 6 meters high and 2 x 2 meters square in cross section. Neutron profiles of the CASTORS are desirable for both content identification and verification. Profile measurements have traditionally been done with He-3 based detectors of about 1 meter high that scan the length of a CASTOR as they are lifted by a crane. Geometric reproducibility errors plague this type of measurement and hence, the ability to simultaneously measure the neutron profile over the entire length of the CASTOR became highly desirable.

Use of the PNNL developed neutron sensitive glass fibers in the construction of a 6-meter high detector was proposed and design/construction of the detector was completed in August 1999. In-house testing was performed and then the detector was shipped to Gorleben, Germany where it was demonstrated on Castors containing PWR fuel in a dry storage site in September 1999. The resulting data show that the detector demonstration was successful.

Acknowledgements

I would like to thank the entire PNNL Euratom Fiber Project Team and congratulate them on winning a well-deserved Outstanding Team Performance Award for their excellent work. The team members include Randy Hansen, Bill Sliger, Rob Workman, Mike Knopf, Deb Barnett, David Stromswold, and the authors.

I would also like to thank the Euratom team members, Peter Schwalbach, Paul De Baere, Herbert Dratschmidt, and Martyn Swinhoe for all their input, guidance, and hard (and often grueling) work. Special gratitude goes to Peter for his labors throughout the entire duration of this project and to Paul for his technical assistance during the testing at Gorleben.

Contents

Introduction

Design Considerations

The glass fiber optic spent fuel neutron profile measurement system is designed to measure the neutron profile of a Castor with high reproducibility and to distinguish spent fuel Castor contents from vitrified waste Castor contents. The basic principle of the detector is that the glass fibers detect thermal neutrons. The glass is loaded with lithium enriched in Li-6, which has a high thermal neutron cross-section. A neutron is captured by the Li-6 and a He-4 and H-3 are created. Because the glass also contains Cerium in a 3^+ ionization state, the excitation caused by the movement of the He-4 and H-3 results in the emission of light from the cerium atoms. This light then travels to the ends of the fiber where it is detected by photon sensitive devices (e.g. photo-multiplier tubes).

In order to measure a profile of the 6-meter high Castors, individual detector elements, arranged end-to-end, had to be used. Since each element must be read out separately with its own channel of electronics, the complexity and cost of the detector increases as the number of elements increase. Thus, the first question that needed to be addressed in the design of this detector was the number of elements necessary to achieve a reasonable profile. A reasonable profile was defined as one in which the fuel burn-up peak in the middle of the profile and the Castor shielding variation at the ends of the profile could be clearly observed for typical Castor contents. Using the information in the Swinhoe[1] paper and results from MCNP modeling we conducted, and determining the cost per element and the percentage of the budget available for glass fiber fabrication and electronics, we chose to use 24 segments (or ribbons) of glass. Each ribbon of glass was made to be 25 centimeters in length by 5 centimeters wide and comprised of a bilayer of glass fibers. This amount of glass results in an expected count rate of 10 Hz to 1 kHz per ribbon for Castor measurements. For details about the glass fibers themselves see References 2-4.

During the course of our MCNP modeling and from the information in the Swinhoe paper, we determined that the gamma flux is at worst about a factor of 30 higher than the neutron flux from the Castor. Because of the inherent insensitivity of the glass to gammas versus neutrons and by setting a relatively high discriminator threshold for neutrons, we can achieve a gamma discrimination level of at least 1:3000. This means that the gamma flux will contribute an error of at most 1% to our neutron measurements. We considered this error to be insignificant.

The neutron background, i.e. neutrons not originating from the Castor being measured, can vary from about 10% - 110% of the neutron flux coming directly from the Castor when measured at about 10 cm from the Castor. By placing additional high-density polyethylene on the back of the detector (for a total of 10 cm), this background flux is reduced by about a factor of 10. The neutron background now results in an error of 1%-10%. In many cases this may be sufficient to extract the desired information out of a measurement (discrimination between spent fuel and waste or a rough verification

measurement). In cases where more accurate measurements are desired, the entire detector can simply be rotated 180 degrees and a background measurement can be taken. This separate background measurement can, in theory, be used exactly as the simultaneous background measurements employed by Swinhoe are used.

The physical detector design consists of a fiber ribbon paired with another ribbon so that each ribbon pair spans 0.5 meters. Four pairs of ribbons are arranged in a 2 meter long high-density polyethylene box that is filled with Gela (see Figure 1). Gela is a gelatinous reenterable encapsulant manufactured by 3M™. The Gela serves to hold the fiber ribbons in place, protect them from atmospheric degradation, and it also acts as a neutron moderator. The poly box slides into a 5" by 2" aluminum extruded box with a flange at both ends. Three of these loaded Aluminium boxes then bolt together to make a total assembled length of 6 meters. Additional poly (~7.5 cm) is attached to the back and sides of the detector to provide background reduction. The flange at the top of the assembly is fitted with three turnbuckles attached to a lifting eye so that the crane can

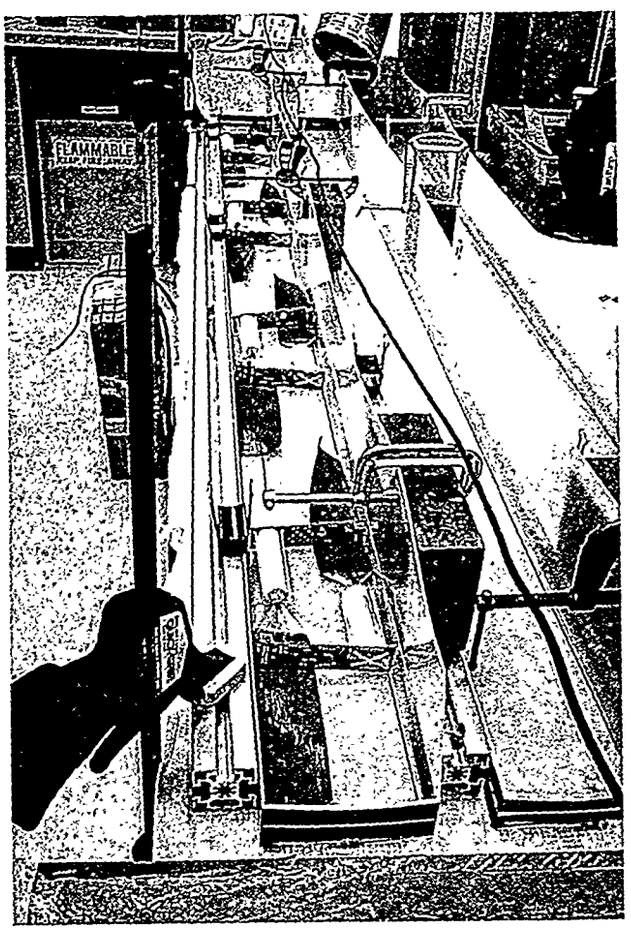

Figure 1 Layout of the eight 25-cm glass fiber ribbons in one of the 2-meter long Gela filled polyethylene boxes. Additional Gela will be added, filling the box and flattening the ribbons. Note that the other two boxes are shown to the right.

lift and support the detector. The mechanics of assembling the detector and aligning the detector vertically was carried out in July of 1999. The fully assembled detector along with the electronics cart is shown in Figure 2. Because the PNNL/Euratom Glass Fiber Optic, Spent Fuel Neutron Profile Measurement System is such a long name, we will henceforth refer to the system as the EFP (Euratom Fiber Project) detector.

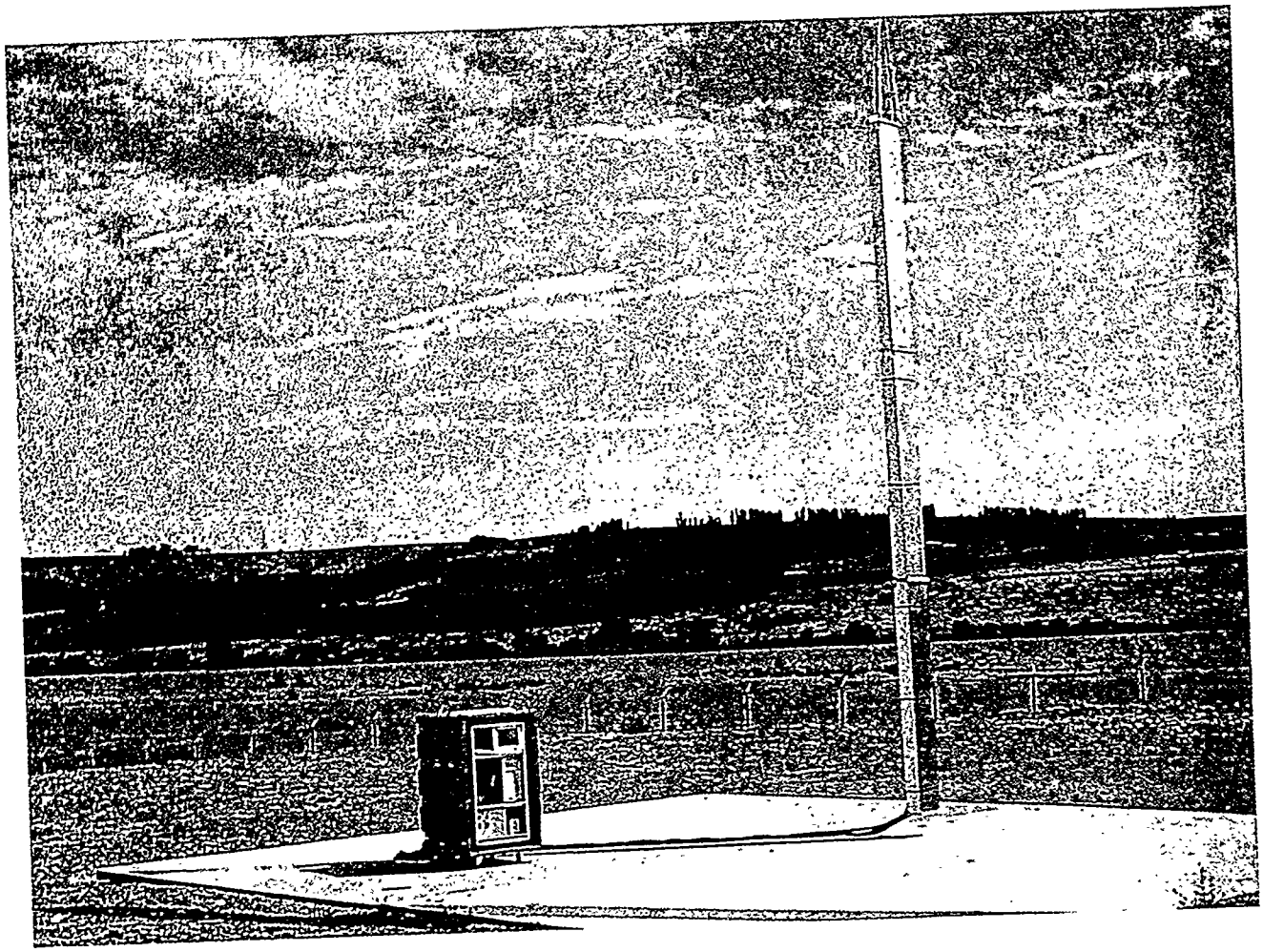

Figure 2 Picture of the assembled EFP detector consisting of three 2-meter long polyethylene boxes each enclosed in aluminum boxes and surrounded with additional polyethylene slabs on three sides. The Columbia River can be seen in the background.

Detector Electronics and Readout

The light in each fiber ribbon is detected by a photo-multiplier tube, PMT, and an ECL logic signal is produced by the amplifier/discriminator boards mounted on the ends of the PMT's. These boards have been used for other fiber projects and needed no further development for this project. Cables running from each board include ECL logic and DC power. All 24 ECL logic signals run to an ECL to TTL converter. The converter boards were designed at PNNL for this specific application. The 24 TTL logic signals then run into two counter boards in a PC running a simple data acquisition/display program designed by TSA Systems ltd. The counters can easily handle a megahertz count rate per channel. Deadtimes of less than 0.1% were seen for the Castor measurements. The acquisition program displays instantaneous and accumulated counts for each channel. The user can input count times, calibration efficiencies, display parameters, filenames, and comments. The data acquisition display screen is shown in Figure 3.

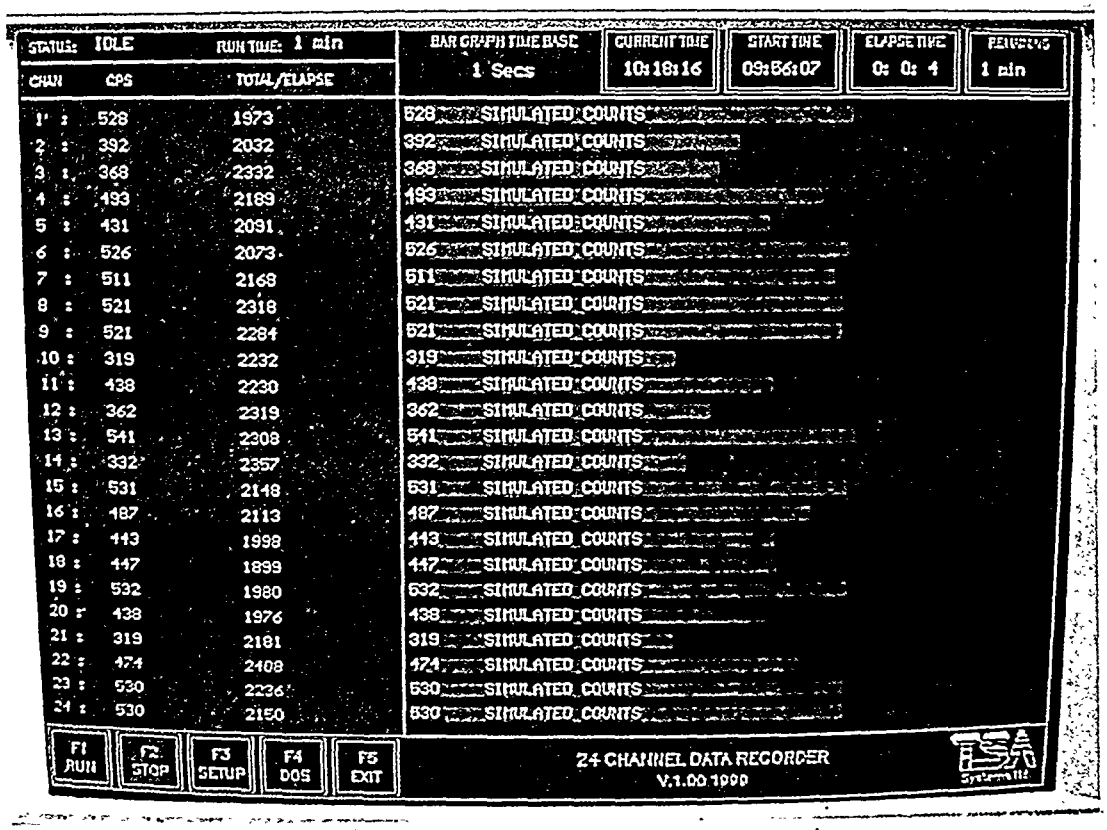

Figure 3 Display of the data acquisition/display program. This particular display is of the demo and hence the words "simulated counts" on the bar graph. The actual program used for taken data in Gorleben was identical in all other respects.

Physical Detector Assembly Details

The assembled detector is 235.79 inches (6 meters) long. The largest cross-sectional dimension is at the flanges which bolt together each section and this dimension measures 11.75" x 6". The polyethylene cross section is 5" x 11". The weight of the assembled detector (all three sections) is less than 500 pounds. The flange at the very top of the detector is fitted with a three-leg turn buckle sling arrangement that allows for vertical leveling adjustments if desired while the detector is suspended.

The device is designed to be lifted by crane and should never come into contact with the ground when assembled. The easiest method for assembly is to lift the first section ~7 feet above the ground, stand the second section on end, and then bolt the two together. The third section is assembled in the same manner (see Figure 4).

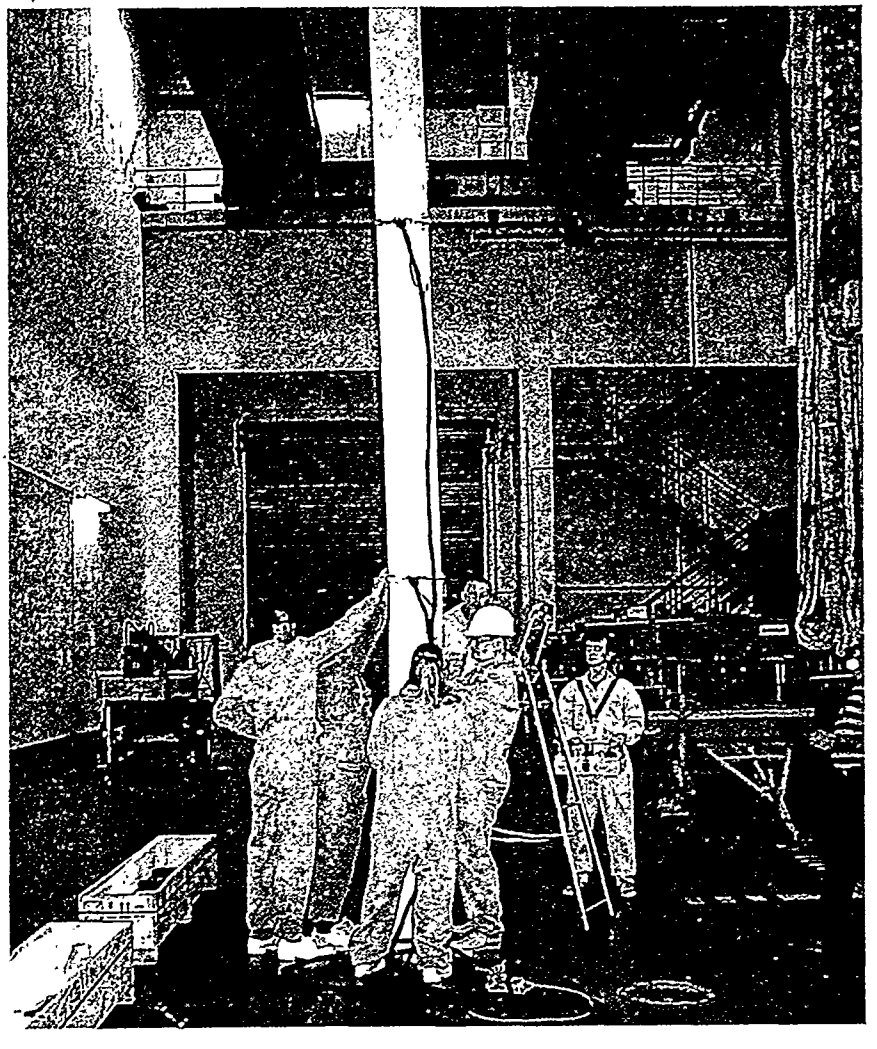

Figure 4 Assembly of the EFP detector in Gorleben, Germany

Each detector section is about 78.6 inches long and is fitted with a square flange plate on both ends. Four allen socket flathead screws, 5/8" in diameter, are used to fasten the top flange of one section to the bottom flange on another. Nuts of 5/8" 316 Stainless Steel are used as well. Cables from each detector run from the detector element to the bottom of each box where they then exit from the front side of the bottom of the flange. As the sections are assembled, the cables from the top sections are fastened to the detector body with tie-wraps or tape (see Figure 4). Disassembly is the reverse process of assembly. The detector can not be laid down horizontally while assembled since it is not engineered to accommodate the stresses that would occur if the three assembled sections were lifted from horizontal to vertical or visa-versa. Engineering of this sort would have added additional weight, time, and money.

Once the entire detector is assembled, the turnbuckles from which the unit is suspended may be adjusted. Adjusting the turnbuckles allows for the leveling of the detector face so that it can be brought very close to the Castor without touching; or barely touching with minimal force. In some cases, it may also be desirable to purposely adjust the detector to hang at a slight angle to remain in contact over the entire length of a surface that is not perfectly perpendicular with the floor. This is the case in many storage facilities since the floor is designed to come to a peak in the middle of the room, allowing for water to run off to the sides where it is collected and drained.

An electronics and computer cart houses all other components of the system not enclosed in the aluminum/poly detector boxes (see Figure 2). This includes the power supplies, logic converters, computer system, and transformers. The cart has dimensions of approximately 30 inches wide, 30 inches deep, and 40 inches tall. The cart has removable wheels and front and back panels. Signal and power cables enter the cart from the back and the operator interface (monitor, keyboard, etc) is located in the front. The cable length allows the cart to be about 10 to 15 feet away from the base of the detector assembly. The system requires that two power cables providing 220 VAC at 50 Hz be plugged into the electronics cart. The electronics cart also houses three small air compressors that provide cooling air to the electronics board of the detector segments. All cables and air hoses leading to the detector assembly are contained in an outer netting jacket that provides for easier cable management. When an overhead crane moves the detector from one area to another after the cables have been connected, it is necessary for a second person to trail with the electronics cart.

Measurements

A facility in Gorleben, Germany was chosen as the test site for the EFP detector because castors containing both spent fuel and vitrified waste are located there. Gorleben is located near the Elbe River (old East-West Germany border) in Northern Germany (see Figure 5). The duties of the Brennelementlager Gorleben mbH (BLG) lie in three areas of waste management. The facility is comprised of a Pilot Conditioning Plant, the Radwaste Storage Facility, and the Transport Cask Interim Storage Facility in which the EFP detector was tested. Figure 6 is an excerpt from a brochure on the site that shows the location of each of these facilities.

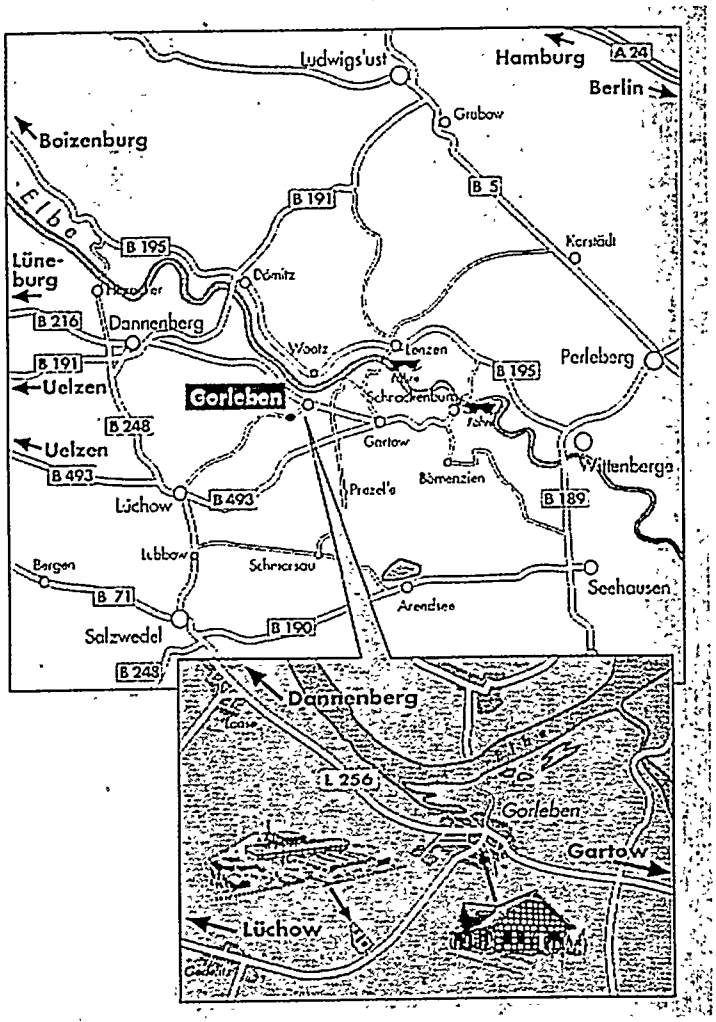

Figure 5 Map showing the location of the BLG facility in Gorleben, Germany.

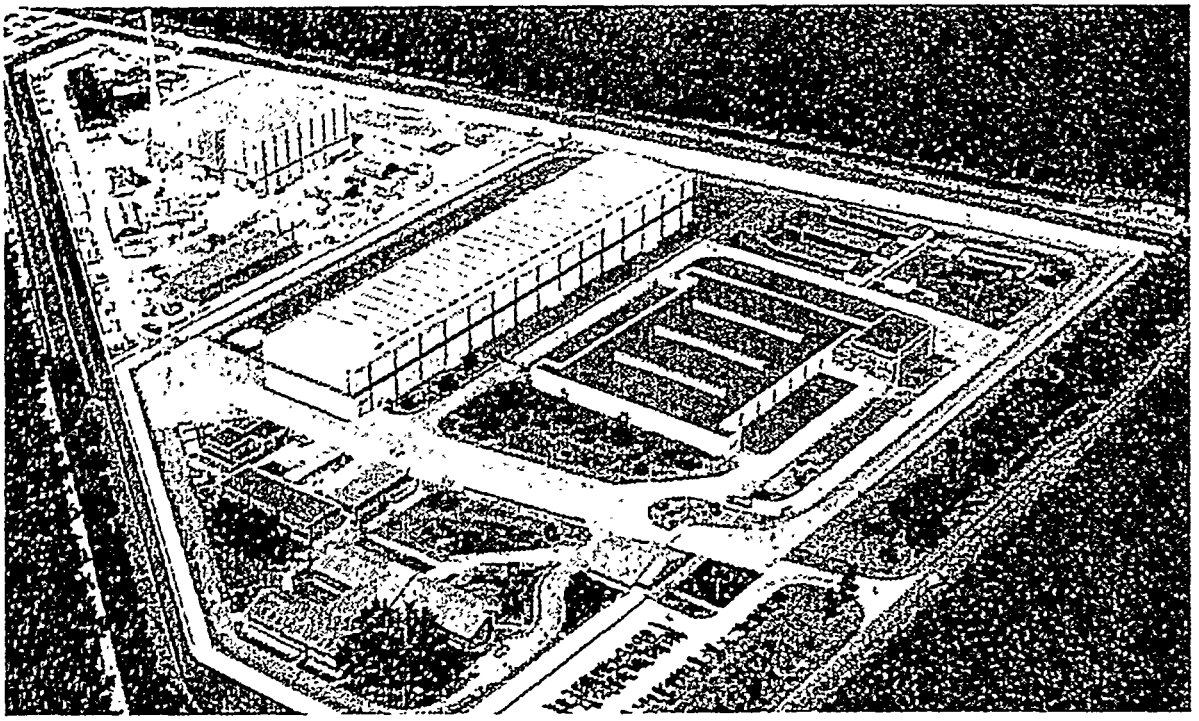

Figure 6 Site map of the facilities at Gorleben. North would be pointing straight up in the picture. The long rectangular building in the middle of the picture is the Transport Cask Interim Storage Facility where testing on the EFP detector was conducted. The large building in upper left of the photograph is the Pilot Conditioning Plant and the I shaped building in the middle of the photo is the Radwaste Storage Facility.

The Transport Cask Interim Storage Facility currently houses six empty castors at the south end of the storage area and eight filled castors at the north end of the storage area. The full ones have either vitrified waste, PWR spent fuel, or BWR spent fuel. Because of time constraints, measurements were carried out only on the castor labeled V19-02, which was loaded with spent PWR fuel. The layout of the castors in the building is shown in Figure 7.

Setup

People involved with the activities which took place during the two days at the BLG were Peter Schwalbach, Paul De Baere, and Herbert Dratschmidt from Euratom, Jose Arenas Carrasco from the IAEA, Dr. Helmut Kuhl from the Wissenschaftlich-Technische Ingenieurberatung GMBH, Krystyna Rudolf from GNS (Gesellschaft fur Nuklear-Services mbH), and Mr. Ehlers from BLG. Mr. Ehlers was our official host and escort. The work on Tuesday was primarily focused on IAEA inspection activities. These activities consisted of visual inspection of seals and also radial (around the circumference) and profile measurements of castors with a He-3 based neutron detector

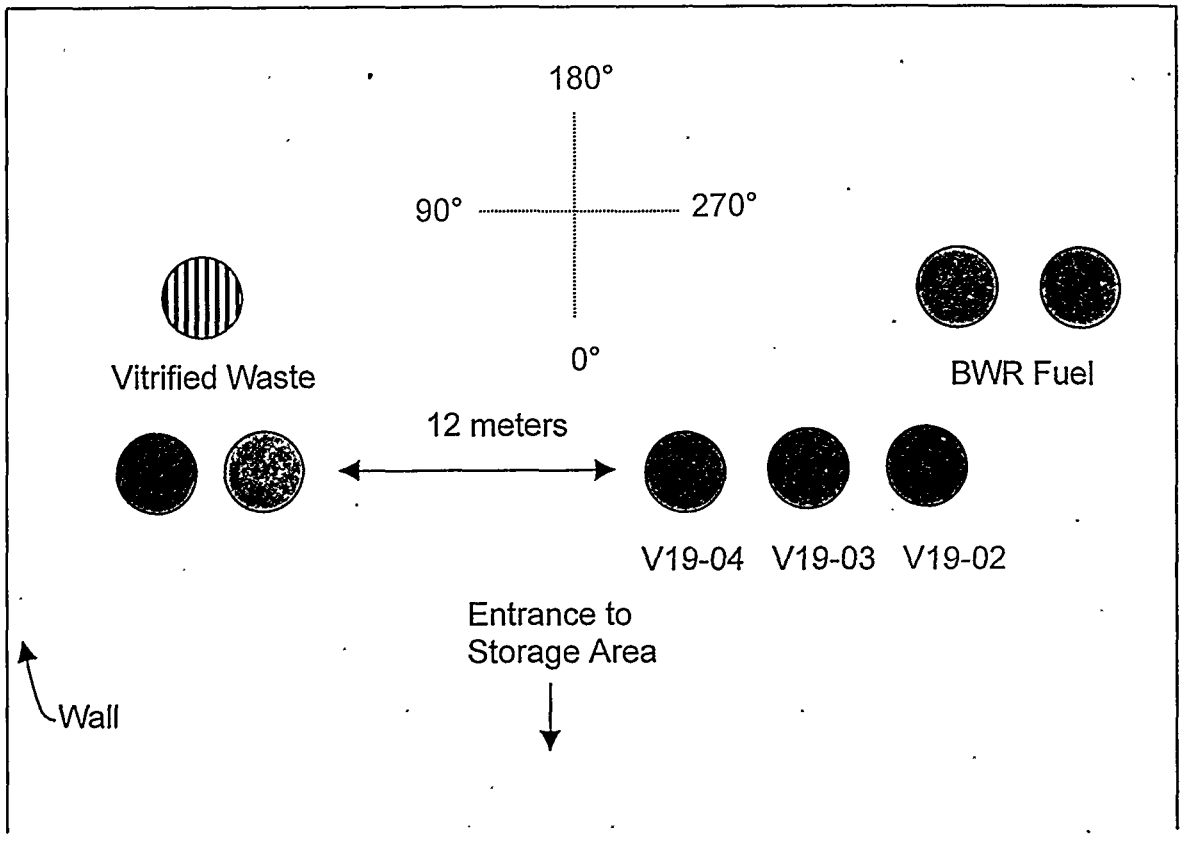

Figure 7 Layout of the Storage area at the Transport Cask Interim Storage Facility at BLG in Gorleben, Germany. The actual colors of the casks are indicated in the drawing.

system called the N50. The N50 detector consists of two banks of 4 He-3 tubes with each bank individually embedded in polyethylene together with Aptek electronics. Additional polyethylene is then inserted between the two banks of He-3 tubes, around the sides, top, and bottom as shown in Figure 7.
The EFP detector was assembled at the end of the workday on Tuesday. Assembly proceeded as described in the Physical Detector Assembly Details section (see also Figure 4).

Data Collection

The detector was moved down to the north end of the storage hall where the castors containing spent fuel and vitrified waste were housed. Once the detector was within about ten meters of the V19-02 castor, we began cabling the detector. After cabling the detector, we powered up the system and looked at the output from each segment. We noticed a trend in the count rates that suggested that one of the high voltage supplies was not putting out the voltage that we expected (both supplies were set at -1100 volts).

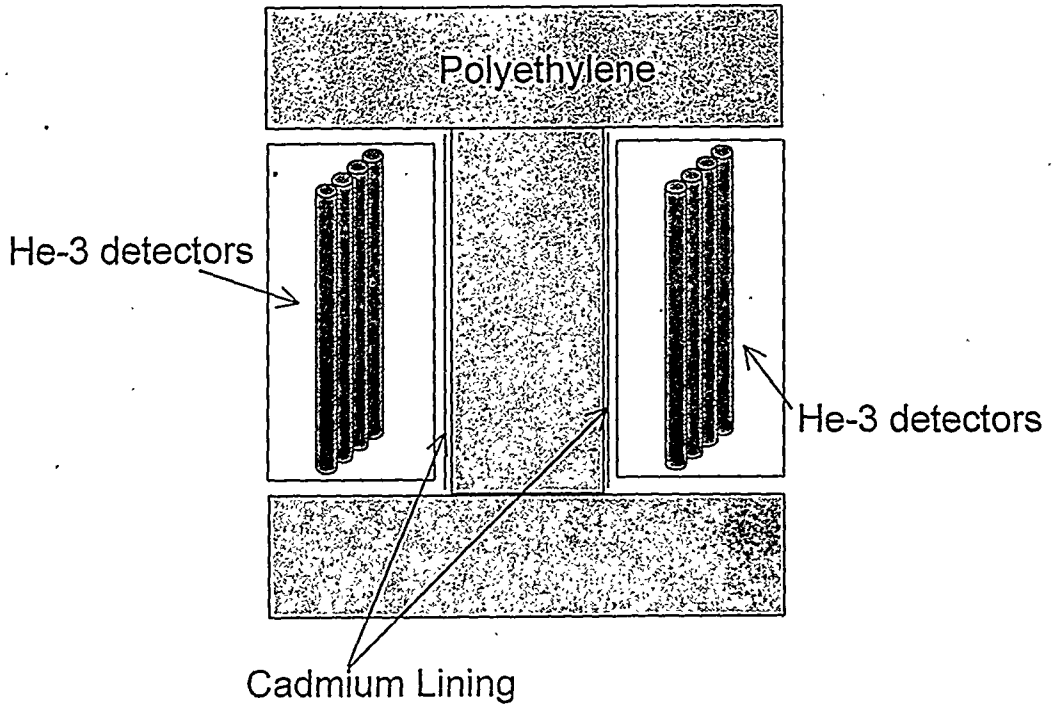

Figure 8 Schematic of N50 detector. The data taken by the N50 is used in the EFP data analysis and for comparison.

Work for the day had to stop at this point and the detector was powered down and left in place for the night. During the discussion later that evening and in the morning, it was decided that when we returned to the storage hall, the first hour of work would consist of examining the output of the high voltage supplies and calibrating the segments for uniform response by using the flat profile region in the middle of the castor which was known from measurement with the N50 system.

Upon returning to the storage hall the next morning, the detector power was restored and we once again looked at the count rate of each segment. During the time we were examining the behavior and output of the high voltage supplies, one of the supplies started smoking. That supply was disconnected from the detector and each group of eight segments was looked at in turn. It was discovered that segment 15 had a short in the high voltage line. It was decided that the most important measurements to obtain were midpoint measurements around the V19-02 castor. By using segments 9,10,11,12,13,14, and 16 this measurement could easily be made. We decided that profile measurements would be made by supplying high voltage to each group of eight segments in turn. Measurements were taken at 0°, 90°,180°,270°, and 315° about the axis of the castor (see Figure 7 for orientation). Generally, measurements at each axial angle were taken with the front of the detector facing the castor and also with the back of the detector facing the castor. Figure 9 shows the detector placement when on contact with the castor.

A table summarizing the actual measurement data collected is given in Appendix 1.

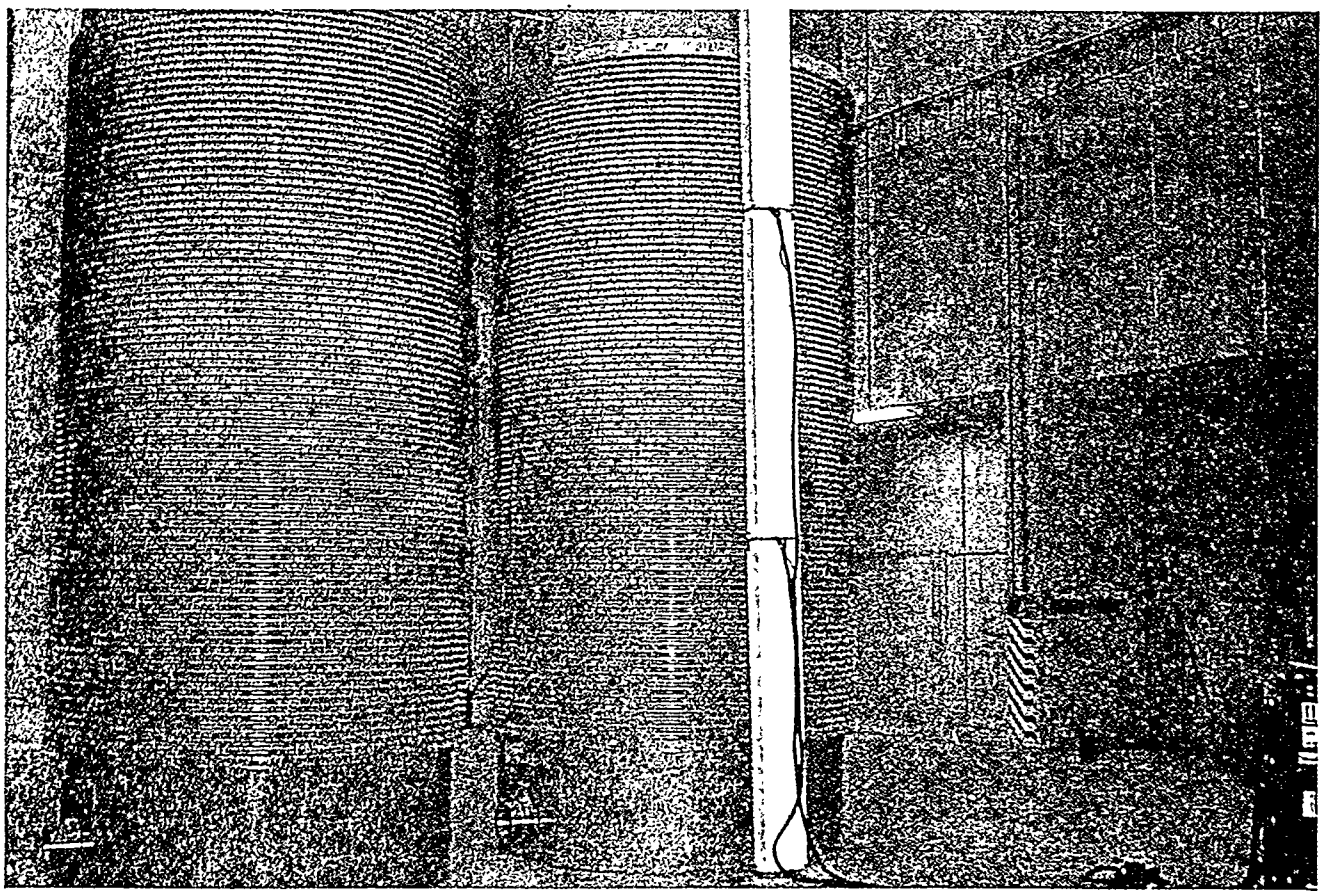

Figure 9 This picture of the EFP detector when it is in contact and facing the V19-02 castor at the 0° position.

Data Analysis

Radial Measurements at Midpoint of Axis

Due to time constraints, a rigorous relative calibration (achieving the same response down the length of the detector in a uniform flux of neutrons) of the 24 detector segments was not performed. Hence, a best effort calibration has to be made from the data that were taken during the measurements. The N50 has a known transmission factor (T) of 0.1. For a given neutron flux entering the front of the N50 detector, the number of neutrons counted in the back He-3 tubes would be 1/10 the number counted in the front He-3 tubes. Since the N50 detector is symmetrical, for a given neutron flux entering the back of the N50 detector, the number of neutrons counted in the front He-3 tubes would be 1/10 the number counted in the back He-3 tubes. Hence, if a flux of neutrons is entering the N50 detector from both sides, the counts in the front and back He-3 tubes can be represented by the following equations:

$$\alpha = F + (T)B \qquad (1)$$

$$\beta = B + (T)F \qquad (2)$$

Where F= the number of counts in the front He-3 tubes due to the neutron flux entering the front of the N50 detector, B= the number of counts in the back He-3 tubes due to the neutron flux entering the back of the N50 detector, α = the total number of counts in the front He-3 tubes, β = the total number of counts in the back He-3 tubes, and T is the transmission factor described above.

At 315°, the back of the detector was facing a wall of the storage facility and no other castors were in line of site. In addition, the flux from the front of the detector is smaller at 315° than at any other angle measured. Given these two conditions, the data from this angle was used to determine a relative calibration of the segments. For the N50 detector we know that the transmission factor is 0.1. We also know for a particular data set (see Appendix 2) that the total number of counts in the front He-3 tubes is 4877, the total number of counts in the back He-3 tubes is 594. With that information we can now determine the relationship between F and B in the equation above:

$$4877 = F + (0.1)B \qquad (3)$$

$$594 = B + (0.1)F \qquad (4)$$

Solving the first equation for F yields F=4877 – (0.1)B. Substituting that expression for F into the second equation and solving for B gives B=107.37 and hence F=4866.26. More usefully,

$$F = (45.31)B \qquad (5)$$

In words, the flux coming through the front of the detector is 45.32 times larger than the flux coming through the back of the detector.

Unfortunately, only three runs were taken with the EFP detector at 315°. Run 13 was at 315°, forward facing, and on contact with the castor. Run 14 was at 315°, forward facing, but with the detector positioned 15 cm from the edge of the cooling fins. Run 15 was at 315°, backward facing with the detector positioned 15 cm from the edge of the cooling fins. In order to determine the transmission ratio, we have to use data from two runs at the same position but with the detector turned by 180°. We now have to assume that for 315° the flux entering the back of the detector in the measurements on contact and at 15 cm from contact (runs 13 and 14) is essentially the same and that the difference in the total count is due to the change in the front flux only. Run 13 had 53,232 total counts while Run 14 had 45,755 total counts (see Appendix 1). The ratio of those two numbers is 0.860 and so in order to relate the N50 ratio above to the EFP data at 15 cm, a correction of 0.860 must be applied yielding:

$$F = 0.860(45.31)B = (38.97)B \qquad (6)$$

The total number of counts in Run 15 was 17,323 and so we can now use the total counts in Runs 14 and 15 to get the following two equations:

$$45755 = F + (T_{EFP})B \qquad (7)$$

$$17323 = B + (T_{EFP})F \qquad (8)$$

Between equations 6,7, and 8 we have three equations with 3 unknowns. Solving for T, the transmission factor for the EFP detector, yields:

$$T_{EFP} = 0.356$$

For every angle at which we have N50 data that we can use to calculate F/B, we can then determine F as measured by the EFP now that the value for T_{EFP} is known. The equation takes the form:

$$F_{EFP} = \frac{\alpha_{EFP}}{\left[1 + T_{EFP}\left(\frac{B_{N50}}{F_{N50}}\right)\right]} \qquad (9)$$

Where F_{EFP} is the number of neutron counts due to the neutron flux entering the front of the EFP detector, α_{EFP} is the total number of neutrons detected in the EFP detector, B_{N50} is the number of counts in the back He-3 tubes due to the neutron flux entering the back of the N50 detector, F_{N50} is the number of counts in the front He-3 tubes due to the neutron flux entering the front of the N50 detector, and T_{EFP} is the transmission factor for the EFP. Using the N50 data in Appendix 2 and Equation 9 above, values for F_{EFP} for the 5 angles measured are calculated as shown in Figure 10.

The comparison of the EFP and N50 data is neither terribly impressive nor unimpressive. The error bars on the EFP data represent statistical errors only and no systematic errors have been added. The overall assumption that taking two runs with the EFP detector facing forward and backward is equivalent to having a symmetrical detector with fibers on the front and the back (such as the N50) may constitute a large systematic error (~10-15%). The assumption described above concerning the relationship of the flux entering the back of the detector when the detector is on contact and at 15 cm from contact may contribute to a significant systematic error as well (~5%). Additionally, it is not "fair" to directly compare the two points in the middle of the graph because the EFP data was taken at 180° while the N50 data was taken at 190°. Since these are the two points of greatest discrepancy, the data without these two points shows good agreement, with the 0° and 90° points having about the same number of counts and the 270° and 315° points representing a decreasing count rate between them. These data, however, show without a doubt that the neutron sensitive glass fibers can do a good job of measuring the neutrons emitted from the castors.

Profile Measurement

Runs 17, 18, and 19 were taken at 0°, facing forward and on contact with the V19-02 castor. Run 18 was taken running segments 1-8. Run 17 was taken running segments 9-16 and run 19 was taken running segments 17-24. In this way, a neutron profile up the entire length of the castor was measured. In order to combine the three runs of data into a single data set, effective relative efficiencies for each segment had to be determined. This had to be done differently for each group of 8 segments. For segments 9-16, Run 22 data (at 0°, forward facing, positioned 7 meters away from the cooling fins) were used and an efficiency factor for each segment was calculated by normalizing to 3000 (see Appendix 3). The number of counts for each segment in Run 17 was then multiplied by these efficiency factors. For segments 17-24, Run 20 data (at 0°, forward facing, on contact, and raised up by 2 meters placing the segments in the middle of the castor where the neutron flux is somewhat flat) were used and an efficiency factor for each segment was calculated by normalizing to 5000 (see Appendix 3). The number of counts for each segment in Run 19 was then multiplied by these efficiency factors. For segments 1-8, there were no other runs from which relative efficiency factors could be calculated. A scaling factor of 0.8 was for the counts in each segment in Run 18 (see appendix 3). The resulting data for all 24 segments are given at the end of Appendix 3.

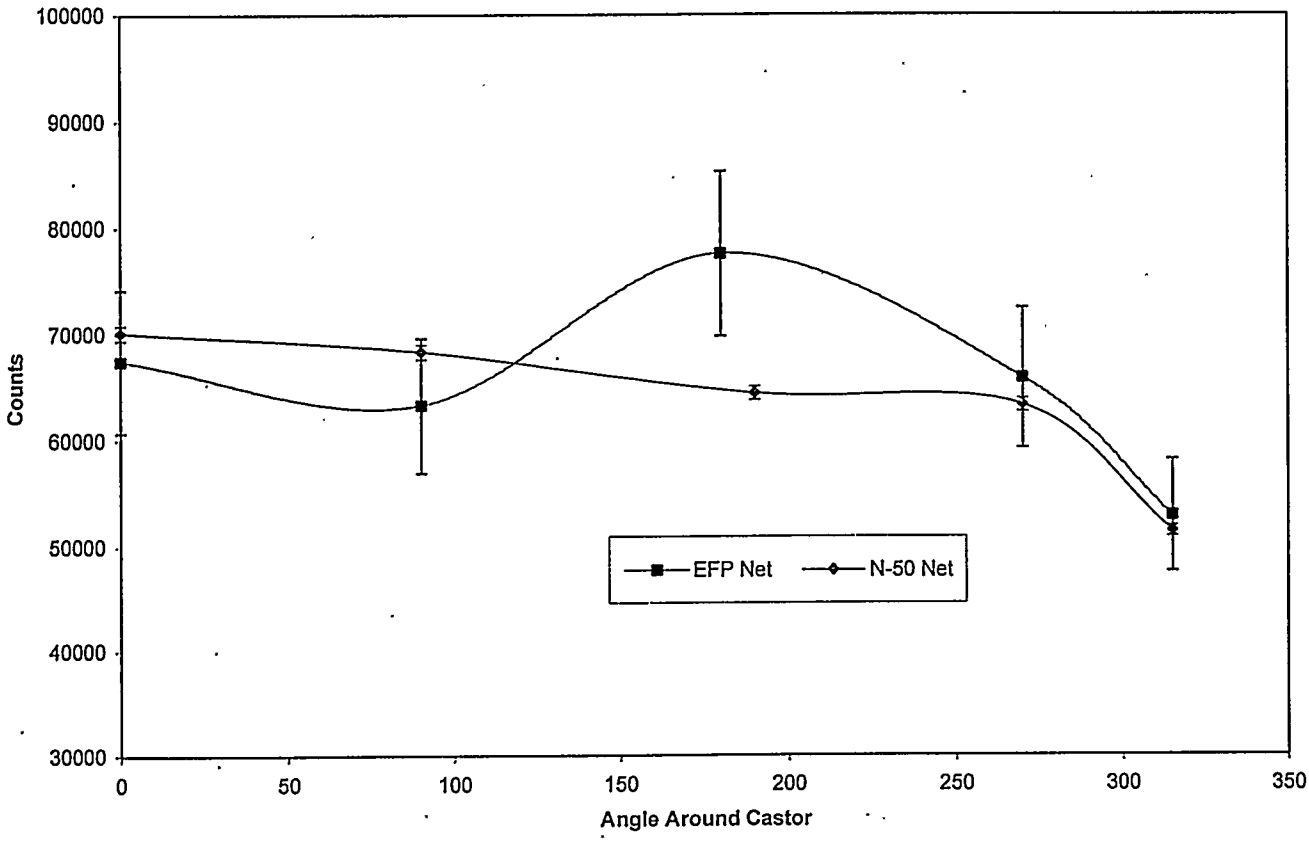

Figure 10 Midpoint measurements on the V19-02 castor with the N50 and EFP detector systems. The N50 data has been normalized for easy comparison.

For comparison to the N50 detector, data from a scanning measurement at 0° were used. The data points for the N50 scan are given as count rates at a given time. In order to compare the EFP data, the total time of the scan was divided in 24 bins, and the midpoint times of each of those 24 divisions were used as the x-values for the EFP data (as opposed to the segment values). The graphical comparison of the data is shown in Figure 11.

The error bars on the data are again only statistical. Possible non-uniformity in the neutron flux in the runs used to determine the relative efficiency factors (Runs 22 and 20) and the fact that a single arbitrary constant was used for normalizing segments 1-8 could contribute to a significant systematic error. Even with the possibility of a non-negligible systematic error aside, the comparison of the EFP to N50 data is quite good. The three-humped characteristic of the neutron profile is clearly visible and the relative amplitude and width of each hump is basically the same for each set of data. Upon closer inspection, there is a difference in the width of the first hump and a slight difference in the width of the third hump. Even taking into consideration possible errors due to picking a midpoint time value from the N50 data to assign an X-value to the segment number of the EFP data for comparison on a single plot, the difference in the widths appear to be real. We suggest that this difference is indicative of the fundamental problem with taking profile measurements with the N50 detector, i.e., operator control of the crane speed over the entire duration of the profile scan. The data seem to indicate that the crane started moving at a given speed and then slowed down slightly and then stayed fairly stable until the last quarter of the scan when it slowed down a bit again.

The profile data shown in Figure 11 is the point of all the work described in this report. It clearly demonstrates the utility and the advantage of using a 6-meter high detector for profile measurements. Additionally, it shows that the neutron sensitive glass fiber optics can perform these measurements very successfully.

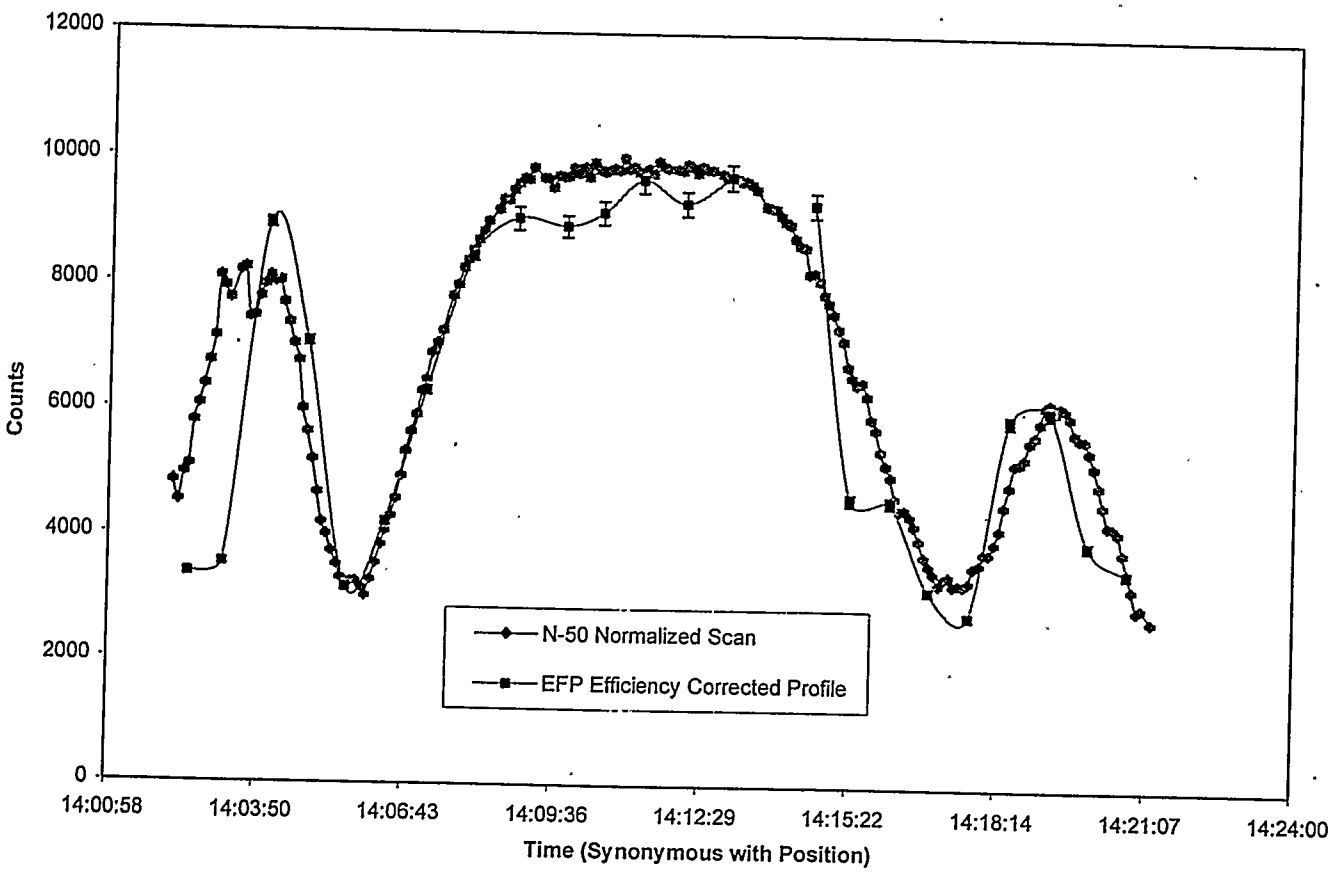

Figure 11 Profile Measurements of the V19-02 Castor at 0 °using the N50 and EFP detectors. The analysis of the data is described in the text. The fifteenth data point is missing for the EFP measurement because that segment was not operating during the profile measurement.

Conclusions

The Euratom Fiber Project based on using neutron sensitive glass fiber optics to develop and demonstrate a 6-meter high detector for measuring the neutron profile of spent fuel dry storage castors is a demonstrated success. The detector was designed, built, and demonstrated in Gorleben, Germany all in 1 year's time. The data resulting from the measurements on the spent fuel castors clearly shows the capabilities and advantages of using the EFP detector for neutron profile measurements.

The minor electrical problems that were experienced were not a detriment to the demonstration in any way. Both Euratom and IAEA seemed generally positive about the performance of the glass and the detector. One area of immediate technical improvement that was discovered was the need for further neutron background reduction by the addition of cadmium in the inside of the detector. Laboratory measurements of the detector stability and the transmission reduction would also be highly desirable. Of more important consequence are the discussions between Euratom and the IAEA that took place in the facility over the course of the two days spent taking measurements there. IAEA stated that it foresaw the detector being transported all over Europe, taking measurements not on a periodic inventory type basis but rather on an "unusual event" type basis (a seal is broken and some level of confidence that the castor contents are unchanged must be established via measurement). Along this same line, IAEA expressed that a measurement at mid height of the castor should be sufficient and that a total neutron profile measurement was not necessary. IAEA, therefore, had a number of critiques about the weight and assembly time of the detector, both of which are completely unavoidable in a six-meter high, fully moderated neutron detector. IAEA also pointed out that the dose to workers could be greatly reduced by much longer cable lengths. Also, Euratom came forth with the statement that they no longer felt that it would be possible to distinguish with confidence the difference between spent fuel and vitrified waste in the castors since both forms of castor contents can vary greatly. In addition, the castors themselves can be made from a variety of companies and are not all of the same design. Hence, it appeared that the consensus was that a six-meter high detector was not needed for the originally targeted purpose. However, Euratom later stated that it felt that a simultaneous full-length castor measurement might still prove desirable in certain inspection scenarios. Discussions of alternate ways to engineer a profile-scanning detector took place.
Ultimately, Euratom and IAEA need to decide whether or not they require a profile detector. If a lighter weight detector is desired, the engineering to accomplish that can easily be carried out.

References

1. D. G. Turner and M. T. Swinhoe, "Neutron Measurements outside Containers of Spent Fuel for Safeguards", published in the proceedings of the 40th annual meeting of the INMM, 1999.
2. K.H. Abel, et al, "Scintillating Glass Fiber Neutron Sensors: I. Production and Optical Characterization", in SCIFI 93 Workshop on Scintillating Fiber Detectors, edited by A.D. Bross, R.C. Ruchti, and M.R. Wayne, World Scientific, New Jersey, pp. 387-394 (1995).
3. K.H. Abel, et al, "Scintillating Glass-Fiber Neutron Sensors," Nucl. Instr. Meth. Phys. Res. A353, 114 (1994).
4. M. Bliss, et al, "Glass-Fiber-Based Neutron Detectors for High and Low-Flux Environments", SPIE, 2551, pp. 108-117 (1994).

APPENDIX 1

Below is a table of the raw data from the V19-02 castor measurements with the EFP detector. The V19-02 castor contains spent PWR fuel.

	Run1								
	V19-2, 0 DEG, FORWARD FACING, ON CONTACT								
Segment	9	10	11	12	13	14	15	16	**SUM**
Counts	10777	11733	10700	10943	10571	11607	0	10576	76907
	Run 2								
	V19-02, 0 DEG, FORWARD FACING, 15 cm FROM COOLING FINS								
Segment	9	10	11	12	13	14	15	16	**SUM**
Counts	9247	10183	9419	9494	9280	10224	0	9184	67031
	RUN 3								
	V19-02, 0 DEG, BACKWARD FACING, 17 cm FROM COOLING FINS								
Segment	9	10	11	12	13	14	15	16	**SUM**
Counts	4119	3972	4080	3674	4150	3645	0	3712	27352
	RUN4								
	V19-02, 270 DEG, FORWARD FACING, ON CONTACT								
Segment	9	10	11	12	13	14	15	16	**SUM**
Counts	9384	9935	9536	9275	9321	9937	0	8968	66356
	RUN 5								
	V19-02, 270 DEG, FORWARD FACING, 15 cm FROM COOLING FINS								
Segment	9	10	11	12	13	14	15	16	**SUM**
Counts	7316	7787	7574	7421	7551	7952	0	7281	52882
	RUN 6								
	V19-02, 270 DEG, BACKWARD FACING, 15 cm FROM COOLING FINS								
Segment	9	10	11	12	13	14	15	16	**SUM**
Counts	3336	3634	3392	3283	3203	3186	0	3257	23291
	RUN 7								
	V19-02, 180 DEG, FORWARD FACING, ON CONTACT								
Segment	9	10	11	12	13	14	15	16	**SUM**
Counts	11292	12265	11776	11594	11461	12004	0	10844	81236
	RUN 8								
	V19-02, 180 DEG, FORWARD FACING, 15 cm FROM COOLING FINS								
Segment	9	10	11	12	13	14	15	16	**SUM**
Counts	10147	11107	10541	10349	10045	10646	0	9786	72621
	RUN 9								
	V19-02, 180 DEG, BACKWARD FACING, 15 cm FROM COOLING FINS								
Segment	9	10	11	12	13	14	15	16	**SUM**
Counts	5285	5762	5331	5284	5018	5422	0	5305	37407

	RUN 10								
	V19-02, 90 DEG, FORWARD FACING, ON CONTACT								
Segment	9	10	11	12	13	14	15	16	SUM
Counts	13541	14935	14032	13480	13544	15180	0	13384	98096
	RUN 11								
	V19-02, 90 DEG, FORWARD FACING, 15cm FROM COOLING FINS								
Segment	9	10	11	12	13	14	15	16	SUM
Counts	12792	14356	13695	13044	13182	14464	0	12558	94091
	RUN 12								
	V19-02, 90 DEG, BACKWARD FACING, 15 cm FROM COOLING FINS								
	ALSO V19-03, 270 DEG, FORWARD FACING, 10 cm FROM COOLING FINS								
	(35 cm SEPARATION BETWEEN CASTORS)								
Segment	9	10	11	12	13	14	15	16	SUM
Counts	14638	16393	15507	15007	14757	16854	0	14451	107607
	RUN 13								
	V19-02, 315 DEG, FORWARD FACING, ON CONTACT								
Segment	9	10	11	12	13	14	15	16	SUM
Counts	7439	8242	7642	7377	7294	8067	0	7171	53232
	RUN 14								
	V19-02, 315 DEG, FORWARD FACING, 15 cm FROM COOLING FINS								
Segment	9	10	11	12	13	14	15	16	SUM
Counts	6422	7178	6634	6304	6178	6874	0	6165	45755
	RUN 15								
	V19-02, 315 DEG, BACKWARD FACING, 15 cm FROM COOLING FINS								
Segment	9	10	11	12	13	14	15	16	SUM
Counts	2510	2804	2542	2382	2402	2293	0	2390	17323
	RUN 16								
	V19-02, 0 DEG, FORWARD FACING, ON CONTACT								
	RUN 16 DATA FILE OVERWRITTEN BY RUN 17. RUN 16 WAS NOT QUITE AS CLOSE								
	IN CONTACT AS RUN 17.								
	RUN 17 IS CONSIDERED SUPERIOR MEASUREMENT TO RUN 16.								
	RUN17								
	V19-02, 0 DEG, FORWARD FACING, ON CONTACT								
Segment	9	10	11	12	13	14	15	16	SUM
Counts	9535	10587	9704	9372	9338	10066	0	9220	67822
	RUN 18								
	V19-02, 0 DEG, FORWARD FACING, ON CONTACT, RUNNING SEGMENTS 1-8								
Segment	1	2	3	4	5	6	7	8	SUM
Counts	4214	4422	11166	8828	3936	5269	7884	10560	56279
	RUN 19								
	V19-02, 0 DEG, FORWARD FACING, ON CONTAC, RUNNING SEGMENTS 17-24								
Segment	17	18	19	20	21	22	23	24	SUM
Counts	4607	5086	3517	3502	7621	6768	4340	4184	39625

	RUN 20								
	V19-02, 0 DEG, FORWARD FACING, ON CONTACT, DETECTOR RAISED BY 2 METERS								
	PUTTING BOTTOM SECTION IN MIDDLE POSITION								
Segment	17	18	19	20	21	22	23	24	SUM
Counts	4980	5536	5553	6325	6443	5578	5512	5998	45925
	RUN 21								
	V19-02, 0 DEG, FORWARD FACING, ON CONTACT, DETECTOR BACK ON GROUND,								
	SEGMENT 9-16								
Segment	9	10	11	12	13	14	15	16	SUM
Counts	9829	10925	9851	9608	9295	10497	0	9406	69411
	RUN 22								
	V19-02, 0 DEG, FORWARD FACING, 7 METERS FROM CASTOR								
	9	10	11	12	13	14	15	16	SUM
	3162	3559	3184	2906	3010	3101	0	2974	21896
	RUN 23								
	V19-02, 0 DEG, BACKWARD FACING, 7 METERS FROM CASTOR								
Segment	9	10	11	12	13	14	15	16	SUM
Counts	1510	1494	1353	1266	1297	1104	0	1347	9371
	RUN 24								
	V19-02, 0 DEG, FORWARD FACING, 15 METERS FROM CASTOR								
Segment	9	10	11	12	13	14	15	16	SUM
Counts	1689	1854	1654	1501	1515	1231	0	1534	10978
	RUN 25								
	V19-02, 0 DEG, BACKWARD FACING, 15 METERS FROM CASTOR								
Segment	9	10	11	12	13	14	15	16	SUM
Counts	706	817	694	615	655	390	0	631	4508

APPENDIX 2

This is the N50 data from the midpoint measurements of the V19-02 castor at the angles also measured with the EFP detector. The numbers are counts/second.

Container	Angle	Front (alpha)	Back (beta)	Front Net (F)
V19-002	0	5,402.21	624.76	5,393.67
V19-002	90	5,900.91	6,989.55	5,254.50
V19-002	190	5,019.15	1,159.18	4,952.76
V19-002	270	4,877.22	594.78	4,866.40
V19-002	315	3,959.58	476.13	3,951.48

APPENDIX 3

The excel spreadsheet data used to calculate the EFP Profile data is given below:

Run 22 at 0 deg and 7 meters			This run is used to calculate relative software efficiency factors for segments 9-16	
		Normilization	Efficiency Factor	Absolute error in Efficiency Factor
9	3162	3000	0.948767	0.016872
10	3559	3000	0.842933	0.01413
11	3184	3000	0.942211	0.016698
12	2906	3000	1.032347	0.01915
13	3010	3000	0.996678	0.018167
14	3101	3000	0.96743	0.017373
15	0	3000	1	
16	2974	3000	1.008742	0.018497
Run 20 det up by 2 meters at 0 deg			This run is used to calculate relative software efficiency factors for segments 17-24	
		Normilization	Efficiency Factor	Absolute error in Efficiency Factor
17	4980	5000	1.004016	0.014227
18	5536	5000	0.903179	0.012139
19	5553	5000	0.900414	0.012083
20	6325	5000	0.790514	0.00994
21	6443	5000	0.776036	0.009668
22	5578	5000	0.896379	0.012002
23	5512	5000	0.907112	0.012218
24	5998	5000	0.833611	0.010764
Run 17 at 0 deg This run is the data for the profile measurement for 9-16				
		Software Effeciency Factor (see Run 22)		Error in Eff. Factor
9	9535	0.948766603	9046.49	0.016872
10	10587	0.842933408	8924.136	0.01413
11	9704	0.942211055	9143.216	0.016698
12	9372	1.032346869	9675.155	0.01915
13	9338	0.996677741	9306.977	0.018167
14	10066	0.967429861	9738.149	0.017373
15	0	1	0	
16	9220	1.008742434	9300.605	0.018497
Run 19 at 0 deg This run is the data for the profile measurement for 17-24				
		Software Efficiency Factor (see Run 20)		Error in Eff. Factor
17	4607	1.004016064	4625.502	0.014227
18	5086	0.903179191	4593.569	0.012139
19	3517	0.900414191	3166.757	0.012083
20	3502	0.790513834	2768.379	0.00994
21	7621	0.776036008	5914.17	0.009668
22	6768	0.89637863	6066.691	0.012002
23	4340	0.907111756	3936.865	0.012218
24	4184	0.833611204	3487.829	0.010764
Run 18 at 0 deg This run is the data for the profile measurement for 1-8				
		Arbitrary Efficiency Scaling Factor		Absolute Error in Corrected Count Value
1	4214	0.8	3371.2	51.93226
2	4422	0.8	3537.6	53.1985
3	11166	0.8	8932.8	84.53544
4	8828	0.8	7062.4	75.16595
5	3936	0.8	3148.8	50.19004
6	5269	0.8	4215.2	58.0703
7	7884	0.8	6307.2	71.03351
8	10560	0.8	8448	82.20949

Run 17 at 0 deg This run is the data for the profile measurement for 9-16					
		Software Effeciency Factor (see Run 22)		Error in Eff. Factor	Absolute Error in Corrected Count Value
9	9535	0.948766603	9046.49	0.016872	185.6476
10	10587	0.842933408	8924.136	0.01413	172.915
11	9704	0.942211055	9143.216	0.016698	186.7368
12	9372	1.032346869	9675.155	0.01915	205.4271
13	9338	0.996677741	9306.977	0.018167	195.0728
14	10066	0.967429861	9738.149	0.017373	200.0048
15	0	1	0		
16	9220	1.008742434	9300.605	0.018497	196.132
Run 19 at 0 deg This run is the data for the profile measurement for 17-24					
		Software Efficiency Factor (see Run 20)		Error in Eff. Factor	Absolute Error in Corrected Count Value
17	4607	1.004016064	4625.502	0.014227	94.55325
18	5086	0.903179191	4593.569	0.012139	89.22103
19	3517	0.900414191	3166.757	0.012083	68.2446
20	3502	0.790513834	2768.379	0.00994	58.31063
21	7621	0.776036008	5914.17	0.009668	100.0917
22	6768	0.89637863	6066.691	0.012002	109.7098
23	4340	0.907111756	3936.865	0.012218	79.89383
24	4184	0.833611204	3487.829	0.010764	70.25427
Run 18 at 0 deg This run is the data for the profile measurement for 1-8					
		Arbitrary Efficiency Scaling Factor		Absolute Error in Corrected Count Value	
1	4214	0.8	3371.2	51.93226	
2	4422	0.8	3537.6	53.1985	
3	11166	0.8	8932.8	84.53544	
4	8828	0.8	7062.4	75.16595	
5	3936	0.8	3148.8	50.19004	
6	5269	0.8	4215.2	58.0703	
7	7884	0.8	6307.2	71.03351	
8	10560	0.8	8448	82.20949	

The results for all 24 segments are listed below:

Segment	Efficiency Corrected Profile Data	Absolute Error
1	3371	52
2	3538	53
3	8933	85
4	7062	75
5	3149	50
6	4215	58
7	6307	71
8	8448	82
9	9046	186
10	8924	173
11	9143	187
12	9675	205
13	9307	195
14	9738	200
15	-	-
16	9301	196
17	4626	95
18	4594	89
19	3167	68
20	2768	58
21	5914	100
22	6067	110
23	3937	80
24	3488	70

Distribution

No. Of Copies

Offsite

4 European Commision

Peter Schwalbach (2)
Martyn Swinhoe (1)
Paul De Baere (1)
Cube Building 009
L-2920 Luxembourg

Onsite

28 Pacific Northwest National Laboratory

Sonya Bowyer (10)
John Smart (4)
Bill Sliger (1)
Rob Workman (1)
Mike Knopf (1)
Deb Barnett (1)
David Stromswold (1)
Ned Wogman (1)
Gordon Dudder (1)
David Roberston (1)
Mary Bliss (1)
Technical Report Files ~~(5)~~ 7